Title
Ligand-Induced Size-Dependent Circular Dichroism in Quantum Dots

Journal
The Journal of Physical Chemistry Letters, 15(31)

ISSN
1948-7185

Authors
Chabeda, Daniel
Gee, Stephen
Rabani, Eran

Publication Date
2024-08-08

DOI
10.1021/acs.jpclett.4c01682

THE JOURNAL OF PHYSICAL CHEMISTRY LETTERS
A JOURNAL OF THE AMERICAN CHEMICAL SOCIETY

pubs.acs.org/JPCL

Letter

Ligand-Induced Size-Dependent Circular Dichroism in Quantum Dots

Daniel Chabeda, Stephen Gee, and Eran Rabani*

Cite This: J. Phys. Chem. Lett. 2024, 15, 7863−7869

Read Online

ACCESS | Metrics & More | Article Recommendations | Supporting Information

ABSTRACT: Recent experiments have probed the chiral properties of semiconductor nanocrystal (NC) quantum dots (QDs), but understanding the circular dichroism line shape, excitonic features, and chirality induction mechanism remains a challenge. We propose an atomistic pseudopotential method to model chiral ligand passivated QDs, computing circular dichroism (CD) spectra for CdSe QDs (2.6−3.8 nm). We find strong agreement between calculated and measured line shapes, predicting consistent bisignate line shapes with decreasing CD magnitude as size increases. Our analysis reveals the origin of bisignate line shapes, arising from nondegenerate excitons with opposing angular momenta. We also explore the impact of chiral ligand orientation on QD surfaces, observing changes in the optical activity magnitude and sign. This orientation sensitivity offers the means to distinguish ordered from disordered ligand configurations, facilitating the study of order−disorder transitions at ligand−QD interfaces.

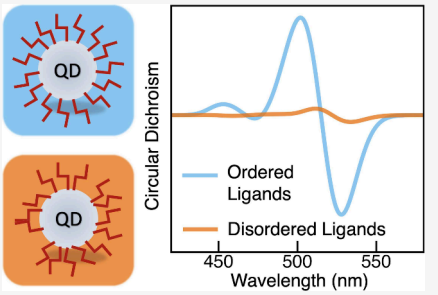

Semiconductor QDs have revolutionized electronic and photonic devices by enabling selective and tunable control of charge and light based on their size.[1−4] A current research frontier is developing sustainably manufactured, highly controllable QDs that exhibit tunable chiroptical properties through their size, shape, and structure, giving access to simultaneous control over charge, light, and spin.[5−10] Such chiral control has been proposed as a tool for enhanced biological imaging, computer vision, and spin-based computing, serving as a motivation to understand the fundamental properties of chiral QDs.[8,11−16]

The CD spectra of QDs show unique features compared with molecular systems. First, the low-energy CD features of chiral ligand passivated QDs appear at optical wavelengths, indicating induction of chirality from the UV-absorbing surface ligands into the excitonic transitions of the NC.[17] Second, each excitonic CD signal vanishes at the absorption maximum wavelength and has a bisignate shape, an observation termed the "derivative" line shape.[18−20] Ben-Moshe et al. proposed that attaching chiral capping ligands to an otherwise achiral QD perturbs the nanocrystal electronic structure, splitting the absorbing exciton into two chiral sublevels, preferentially excited by opposite circular polarizations.[18] No theoretical examination of this proposed chirality-induced degeneracy lifting has been offered in the literature, to the best of our knowledge, mainly because calculating accurate excited states in nanoscale systems of experimentally relevant sizes remains a computational challenge. Dipole-coupling models have been used to theoretically predict the magnitude of optical activity for nanocuboids,[21−24] and a recent work utilized first-principle methods to compute chiroptical spectra of a 1.9 nm CdSe QD.[17] Additional insights from theory are required to clarify the interplay of ligand structure and chiroptical properties in chiral QDs, and specifically, it is necessary to develop computationally efficient methods that are capable of capturing the atomistic structure that generates a chiroptical response while scaling modestly with system size.

To address this, we use the atomistic semiempirical pseudopotential approach to calculate circular dichroism spectra of CdSe QDs of relevant sizes, achieving excellent agreement with the experimental results. Our results indicate that the excitonic peaks are not split into angular momentum sublevels by the chiral ligand field. Instead, neighboring excitonic transitions with differently signed angular momenta produce transitions with opposing rotational strength, and the CD line shape depends on the competing contributions from many transitions across the entire spectrum. Beyond investigating the excitonic origin of the derivative line shape, we apply our molecular level control over individual ligands to investigate orientation dependence. We find that the CD line shape is sensitive to the orientation of chiral surface ligands, exhibiting angle-dependent and anisotropic peak intensities, and show that incorporating increased ligand disorder in ensemble averaged conditions leads to cancellations that attenuate the CD signal by up to 3 orders of magnitude.

Received: June 5, 2024
Revised: July 17, 2024
Accepted: July 19, 2024
Published: July 25, 2024

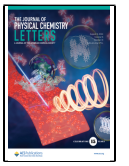

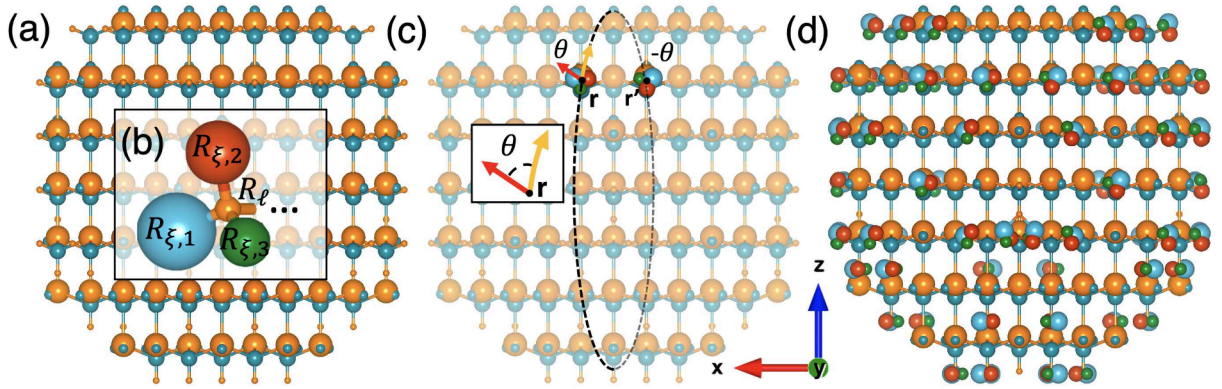

Figure 1. (a) Achiral 2.6 nm CdSe QD with our standard passivation ligand potentials (small orange and blue spheres) as viewed down the [010] axis. (b) Geometry of a CLP: the passivation potential attached to an undercoordinated Cd atom, $\mathbf{R}_l$, becomes a stereocenter through the placement of three nonequivalent Gaussian potentials represented pictorally as blue, red, and green lobes. (c) Addition of a chiral ligand potential (CLP) with orientation angle θ, where θ is the in-plane angle between a vector from the CLP center to its strongest lobe (inset: red arrow) and a geodesic toward the north pole (inset: gold arrow). To eliminate undesired structural asymmetry, we add a CLP with angle $-\theta$ across the 2-fold symmetry plane, and all ligands are positioned in such pairs. (d) Mirror-symmetric CLPs are placed on the QD to generate the reported CD spectra.

A fundamental understanding of ligand order is central to optimizing properties of QDs because favorable optoelectronic properties are typically achieved through surface passivation.[18,20,25−32] Ligand shell ordering impacts the QD growth, solution-phase stability, optical blinking rates, and radiative lifetimes, making the study of ligand organization of great technological and fundamental interest.[33−39] However, probing the order−disorder transition experimentally has required intensive techniques such as sum-frequency generation,[40−42] X-ray photoelectron spectroscopy,[42] powder X-ray diffraction,[43] and NMR.[41,44] These techniques enable the assessment of relative orientation, either through a signal that requires inversion symmetry breaking or by spatially resolving the 3D chemical environment. Optical activity is a phenomenon that is sensitive to inversion symmetry breaking of chiral systems and has the potential to be employed as a less intensive method to study collective ligand orientation on QDs.[45,46] To the best of our knowledge, no experimental analyses of ligand orientation and order through optical activity measurements have been reported. In this report, in addition to uncovering the relation between the exciton structure and the CD response, we also highlight the possibility of CD to probe *in situ* ligand order.

In order to describe the quasiparticle properties, we use the atomistic semiempirical local pseudopotential model,[47] with a Hamiltonian, $\hat{h}_{QP}(\mathbf{r})$, given by

$$\hat{h}_{QP}(\mathbf{r}) = -\frac{1}{2}\nabla_{\mathbf{r}}^2 + \sum_{\alpha} v_{\alpha}(|\mathbf{r} - \mathbf{R}_{\alpha}|) + \sum_{l} v_{l}(|\mathbf{r} - \mathbf{R}_{l}|) + \sum_{\xi} v_{\xi}(\mathbf{r}) \tag{1}$$

where α indexes the atom centered at position $\mathbf{R}_{\alpha}$ with a pseudopotential $v_{\alpha}(|\mathbf{r} - \mathbf{R}_{\alpha}|)$, l indexes the passivation ligand at position $\mathbf{R}_l$ with potential $v_l(|\mathbf{r} - \mathbf{R}_l|)$, and ξ indexes the chiral ligand potential (CLP) with potential $v_{\xi}(\mathbf{r})$. The atom-centered pseudopotentials depend on the atom type, and for atom type μ, it is given in reciprocal space by[48,49]

$$\tilde{v}_{\mu}(\mathbf{q}) = \frac{a_{0,\mu}(q^2 - a_{1,\mu})}{a_{2,\mu}\exp(a_{3,\mu}q^2) - 1} \tag{2}$$

In eq 2, q is the reciprocal lattice vector and the $a_{i,\mu}$ are atom-specific parameters (tabulated in the Supporting Information) fitted to reproduce the bulk band structure, band gaps, effective masses, etc. We also use ligand pseudopotentials, $v_l(|\mathbf{r} - \mathbf{R}_l|)$, to passivate surface atoms with dangling bonds (Figure 1a).[50] The procedure to place the ligand potential at position $\mathbf{R}_l$ is described elsewhere.[47]

Since explicit description of the chiral ligand molecules is computationally unfeasible, to induce chirality, we add to the aforementioned passivation potentials a layer of chiral ligand pseudopotentials (CLPs). We take a simple form for these potential functions: a tetrahedral arrangement of three nonequivalent Gaussian functions (Figure 1b)[51]

$$v_{\xi}(\mathbf{r}) = \sum_{i=1,2,3} a_i \exp(-b|\mathbf{r} - \mathbf{R}_{\xi,i}|^2) \tag{3}$$

where i indexes the three lobes of CLP ξ, each centered at $R_{\xi,i}$, needed to form a tetrahedron around passivation ligand $\mathbf{R}_l$ (see Figure 1b). The values of a_i and b are knobs that tune the magnitude and dissymmetry of induced optical activity in our model (see the Supporting Information). Small amplitudes a_i were used such that the CLPs only weakly perturb the QD electronic structure, generating circular dichroism without significantly changing the band gap or quasiparticle energies (see the Supporting Information).

We define the orientation of a CLP around the central ligand at position $\mathbf{R}_l$ by an angle, θ, the in-plane angle between the vector from $\mathbf{R}_l$ to the strongest lobe of the CLP (Figure 1c red arrow) and the vector along the geodesic from $\mathbf{R}_l$ toward the positive z pole (Figure 1c gold arrow). This angle functions as a dihedral that controls the simultaneous rotation of the three CLP lobes about the $\mathbf{R}_l$−Cd bond axis. The choice of angle reference is arbitrary, but defining the angles with respect to a geodesic geometry takes account of the natural spherical symmetry of the QDs.

Introducing chiral ligands induces optical activity through the stereochemistry of the CLP. Additionally, because we perform calculations on a single QD rather than an ensemble, any other rotoreflection symmetry breaking will also induce optical activity. For example, an unintended "structural chirality" can arise from asymmetric placement of ligands across the σ_v plane of the CdSe QD. This structural contribution is canceled out over ensemble experimental measurements but must be delineated and removed for calculations of individual QD particles. Computational works where this effect is not

https://doi.org/10.1021/acs.jpclett.4c01682
J. Phys. Chem. Lett. 2024, 15, 7863−7869

considered should carefully interpret the contributions from ligand stereochemistry vs structural symmetry breaking.[17,20,52]

To obtain a CD spectrum that captures ligand-induced chirality and excludes structural asymmetry, we place the CLPs in pairs across the σ_v mirror plane, while enforcing consistent stereochemistry. The ligands on each side of the plane are given opposite orientation angles θ and $-\theta$, respectively (Figure 1c). By enforcing the same stereochemistry for ligands on both sides of the mirror plane, the ligand-induced chirality persists even as structural asymmetries are eliminated (Figures S2−S6). We fully passivate the surface of the QD by populating half of the QD with CLPs oriented with angle θ and the opposite half with CLPs of angle $-\theta$. Sites where passivation would lead to steric clashing of the CLPs were left unpassivated (Figure 1d).

With our model Hamiltonian, we use a real-space grid representation and the filter-diagonalization technique[53,54] to obtain valence and conduction band edge quasiparticle eigenstates with energy errors converged to within 10^{-3} meV. The excitation energy of each electron−hole pair was corrected to first order in the electron−hole interaction,[55] and the optical absorption spectra were then calculated in the dipole approximation:

$$\varepsilon(\omega) = \frac{8\pi\omega}{\hbar c} \sum_{a,i} \delta(\omega - \omega_{ai}) |\boldsymbol{\mu}_{ai}|^2 \tag{4}$$

where c is the speed of light, ω_{ai} is the correlated excitation energy of exciton $|a\rangle \otimes |i\rangle$ having an electronic transition dipole given by

$$\boldsymbol{\mu}_{ai} = \langle a|\mathbf{r}|i\rangle \tag{5}$$

Similarly, the circular dichroism spectra, $\Delta\varepsilon(\omega) = \varepsilon_L(\omega) - \varepsilon_R(\omega)$, were calculated using the equation of Rosenfeld for a collection of randomly oriented chiral molecules[56]

$$\Delta\varepsilon(\omega) = \frac{16\pi\omega}{3\hbar c} \sum_{a,i} \delta(\omega - \omega'_{ai}) \, \mathrm{Im}[\boldsymbol{\mu}_{ai} \cdot \mathbf{m}_{ia}] \tag{6}$$

where

$$\mathbf{m}_{ai} = \langle a| - \frac{1}{2}\mathbf{L}|i\rangle \tag{7}$$

is the magnetic transition moment from stat$|i\rangle$ to state $|a\rangle$ and $\mathbf{L}$ is the orbital angular momentum. The quantity $\mathrm{Im}[\boldsymbol{\mu}_{ai} \cdot \mathbf{m}_{ia}]$ is the rotational strength of the transition. The Dirac delta function in the preceding equations is approximated by a Gaussian line shape broadened by 50 meV, consistent with the experimental inhomogeneities and finite temperature effects.[57] For an elucidation of the excitonic features of states generated by this pseudopotential approach, see the work of Zunger, Rabani, and collaborators.[47,58−60]

We apply the described electronic structure model to compute CD spectra for chiral CdSe QDs with diameters of 2.6, 2.9, 3.4, and 3.8 nm that are comparable to experimental measurements.[18,52] Figure 2 shows a comparison between theoretical and experimental absorption (panels a and b) and CD (panels c and d) spectra. We focus on optical transitions that give rise to low-energy features in the CD spectra.

As can be seen in Figure 2 a,b, we find very good agreement of the absorption onset comparing the measured and calculated spectra for the range of QD sizes considered, and we do not use any scaling parameters. This agreement is expected based on previous validations of the semiempirical pseudopotential approach[47] but does not necessarily extend to calculation of

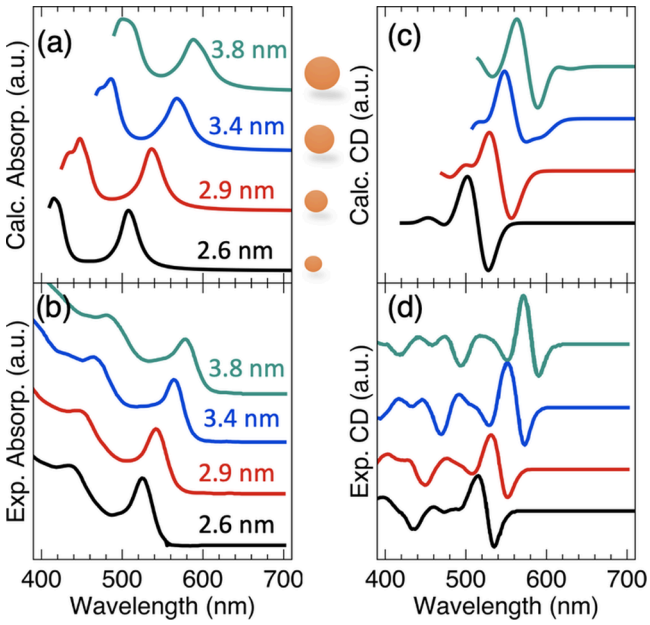

Figure 2. Absorption spectra from theory (a) and experiment (b) as well as CD spectra from theory (c) and experiment (d) for 2.6 nm (black), 2.9 nm (red), 3.4 nm (blue), and 3.8 nm (teal) CdSe QDs. We quantitatively capture the red-shift with increasing system size and bisignate line shape of CD at the low-energy excitonic transitions. CD magnitudes have been normalized to appear on the same scale.

the CD response. The agreement in comparison to experiments[18] shown in Figure 2c,d suggest that the semiempirical pseudopotential model can also capture the features at the onset of CD response in QDs, which is not a trivial result. Our model quantitatively recovers the consistent bisignate line shape observed in CD measurements as well as its red-shift with increasing system size.[18] This agreement suggests that the CD response is sufficiently described by our ligand potential approach. Additionally, as we do not include any structural distortion to the QD in our model, this agreement suggests that induced chirality can be understood by an electronic coupling mechanism.

Discrepancies in the size-dependent behavior have been reported in the literature,[20,25] and we applied our model to investigate the relationship between QD size and CD strength. Contrary to the increasing absorption trend with size,[61,62] we find that the CD intensity decreases with increasing QD size.

The CD response was compared between dot sizes by calculating the dissymmetry, $g(\omega)$, a measure of optical activity that is scaled by the absorption strength

$$g(\omega) = \frac{\Delta\varepsilon(\omega)}{\varepsilon(\omega)} \tag{8}$$

where ω is the incident frequency, and the total absorption includes contributions from magnetic dipole transitions. A decrease in $g(\omega)$ could arise due to a decrease in $\Delta\varepsilon(\omega)$, an increase in $\varepsilon(\omega)$, or the simultaneous increase of both with a steeper increase in $\varepsilon(\omega)$. The absorption coefficient scales with the QD diameter, increasing due to the increase in wave function overlap for larger QDs. The differential absorption coefficient, $\Delta\varepsilon(\omega) = \varepsilon_L(\omega) - \varepsilon_R(\omega)$, does not obey a similar trend but decreases with increasing QD size (Figure 3). Even though the individual coefficients of absorption for left- and right-handed light would increase with QD size, their difference depends on

https://doi.org/10.1021/acs.jpclett.4c01682
J. Phys. Chem. Lett. 2024, 15, 7863−7869

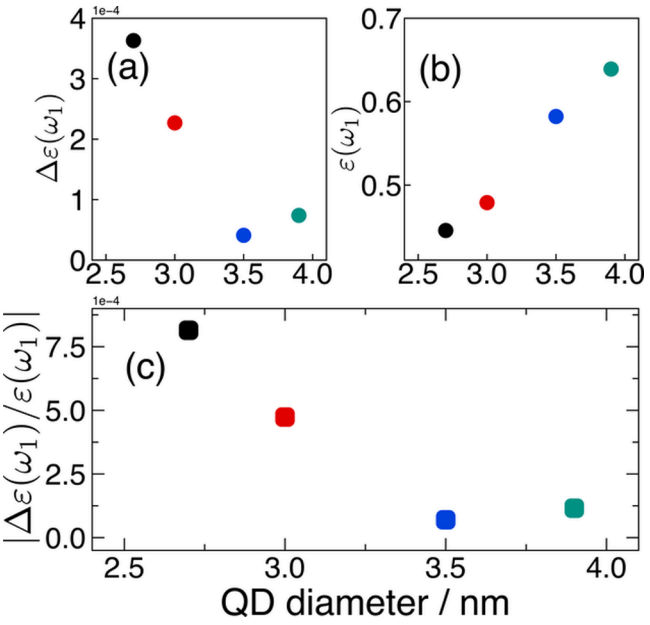

Figure 3. Dissymmetry factors, $g(\omega_1) = \Delta\varepsilon(\omega_1)/\varepsilon(\omega_1)$, where ω_1 is the frequency of the first CD extrema, plotted against the QD diameter. Panel a shows the size-dependent trends in CD, while panel b shows absorption. Panel c gives the size-dependent *g*-factors. The observed decrease in dissymmetry with size is due to the decrease in CD strength and increase in absorption strength with QD diameter. The absolute magnitude of $g(\omega)$ is arbitrarily controlled by our choice of CLP strength and not associated with any specific molecular identity.

the rotatory power of the wave functions involved in the electronic transition. A nonzero rotatory strength is induced by the chiral ligands on the surface of the QD. For small QDs, perturbation by the chiral ligand potentials has a large, asymmetric influence on the shape of the QD wave functions, leading to a large CD magnitude. For large QDs, the chiral ligand potentials on the surface have a relatively weaker influence on the overall asymmetry of the interior QD wave functions because the perturbing ligands are small compared to the total wave function. This can be interpreted in terms of the surface-to-volume ratios for small and large QDs, where the decreasing surface-to-volume ratio with increasing QD diameter means less influence from the surface ligand perturbation on the total wave function dissymmetry.

A puzzling observation in early chiral QD experiments was the bisignate (derivative) line shape of their CD spectra,[18] very distinct from the CD spectra of molecules, which typically show maxima at the absorption peak. Equipped with the theoretical tools to investigate CD features from individual excitonic contributions, we first assessed the hypothesis of chirality-inducing exciton splitting. It has been proposed that the bisignate line shape is due to degeneracy lifting of exciton levels under a chiral ligand field, with oppositely polarized magnetic dipole transitions. This phenomenon would lead to neighboring oppositely signed peaks and result in the bisignate shape characteristic of chiral ligand passivated QDs.

The calculated excitonic energies, however, show little evidence of this when comparing achiral and chiral QDs. Figure 4 shows that the exciton level structure for several low-lying states is minimally affected by the introduction of chiral ligand potentials. A small degeneracy breaking of the first two excitonic levels is observed due to symmetry lowering in the chiral structure. However, the energy splitting is not sufficient to

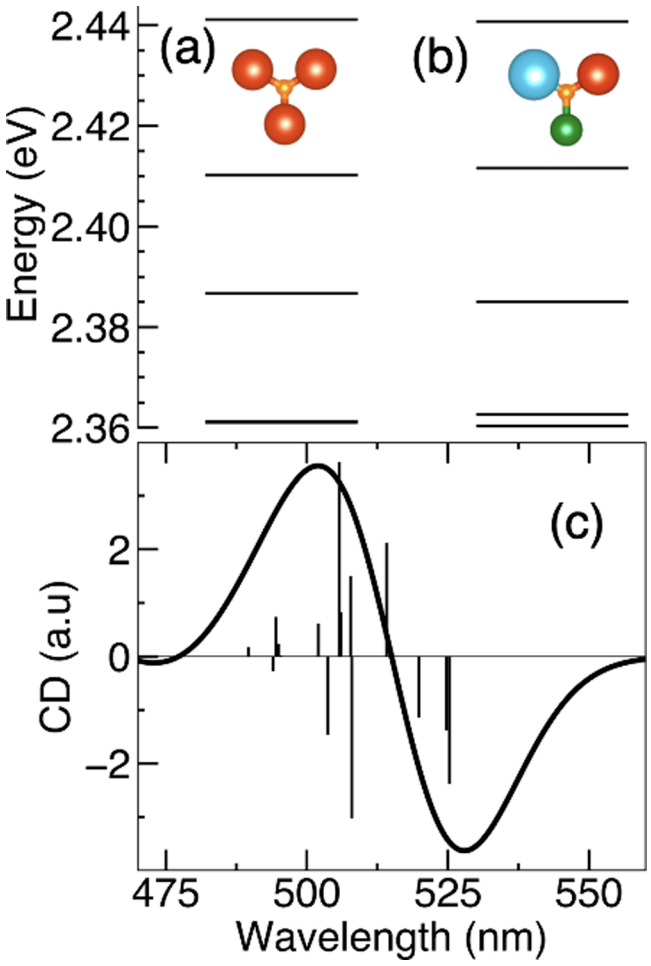

Figure 4. Exciton energy levels for (a) an achiral and (b) a chiral 2.6 nm CdSe QD. The achiral dot was prepared using the intermediate strength potential at all tetrahedral positions so that the energy scale of the two Hamiltonians were equivalent. The excitonic states are analogous; a small degeneracy breaking of the first two excitonic levels is observed due to a symmetry lowering in the chiral structure. However, the energy splitting of the symmetry breaking is not sufficient to explain the bisignate line shape. Additionally, the rotational strengths of those states are both negative, yielding the same preference of circularly polarized light. (c) CD spectra with associated rotational strength sticks for the chiral 2.6 nm QD.

explain the location of the two peaks in the bisignate line shape. Additionally, the rotational strengths of those states are both negative, yielding the same preference of circularly polarized light. Our model suggests that the observed line shape emerges from contributions of many transitions of opposing angular momenta (Figure 4c, black line). This behavior emerges from the high density of excitations, differing from the behavior of small clusters and molecules.

The competing effect of positive and negative contributions means that the wavelength of each derivative peak does not align with the absorption maximum. As further discussed below, modulating the magnitude of the rotational strengths by rotating the chiral ligands shifts the position of the apparent CD extrema; see Figure 5 below for further analysis.

The atomistic control leveraged in our model lends itself to studying the impacts of the ligand orientation on the CD spectra. To explicitly study the impact of ligand orientation on CD features, we generate configurations where all chiral ligands are

https://doi.org/10.1021/acs.jpclett.4c01682
J. Phys. Chem. Lett. 2024, 15, 7863−7869

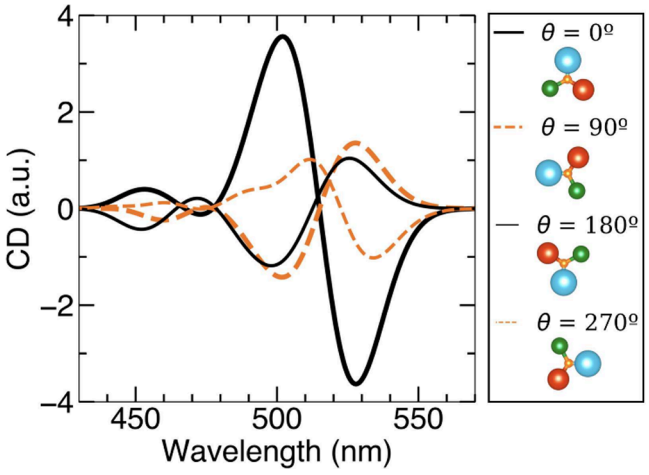

Figure 5. CD spectra of 2.6 nm CdSe QDs with chiral ligand potentials oriented with relative angles of 0° (thick black), 90° (thin black), 180° (thick orange), and 270° (thin dotted orange). The spectra reveal strong orientation dependence of the CD signal, with ligand rotations inducing magnitude, sign, and peak wavelength changes. The flipped ligand orientations, $\Delta\theta = 180°$, do not show flipped CD spectra because the asymmetry of chiral ligands enforces a directionality that makes all orientations unique.

oriented with the same angle θ as defined previously. We illustrate the orientation dependence for a QD with a diameter of 2.6 nm, finding qualitatively similar results for large QDs and nanorods (Figures S7 and S8).

Figure 5 shows four representative CD spectra with different relative ligand orientations. The line shapes show a clear dependence on the chiral ligand potential (CLP) angle, with complete inversion of the chiral signal possible through merely a collective ligand rotation. Notice that flipping the chiral ligand from 0° (thick black) to 180° (thin black) does not produce the mirror image CD signal. Similarly, the 90° (thick dotted orange)/270° (thin dotted orange) pair does not exhibit mirrored spectra. That is because these complementary orientations are not mirror symmetric: there are no possible rotations that exactly invert the stereochemistry of a chiral ligand. Chirality enforces asymmetry, so that all rotations are unique.

This directional asymmetry is crucial to understand experiments, where intuition might expect that ensemble distributions of ligand orientations could lead to cancellation of the CD signal. We anticipate that the CD signal will not completely cancel even under isotropic rotations of an ensemble of ligands because the rotational strength depends anisotropically on ligand orientation. This will play a significant role in determining the average CD response of an ensemble of randomly oriented chiral ligand passivated QDs. In addition, we find that the CD line shape of a single configuration is extremely sensitive to the ligand orientation. Modulating the ligand orientation changes the sign of the Cotton effect, shifts the apparent location of each bisignate extrema by up to 20 nm, and results in trisignate rather than bisignate features (see Figure S7). Our main takeaway is that the CD line shapes of QDs are not intrinsic to the identity of the chiral ligand inducer, but rather the line shape is flexibly determined by the relative orientation of the perturbing ligand potential and QD electronic transitions.

The sign flips and magnitude changes are understood from the behavior of the underlying transitions. To build this understanding from a simple conceptual picture, we consider the rotatory strength of uncorrelated electron−hole pairs. In this limit, a single transition will contribute a rotational strength proportional to $\boldsymbol{\mu}_{ai}\cdot\boldsymbol{m}_{ia} = \mu_{ai}m_{ia}\cos\phi$ as given by eq 6 for an electron in quasi-state a and a hole in quasi-state i. The linear dipole transition moment depends on the overlap of an electron in state $|a\rangle$ and a hole in state $|i\rangle$, and the magnetic transition moment depends on the orbital angular momentum component between $|a\rangle$ and $|i\rangle$. The angle ϕ is the relative angle between those transition moment vectors.

We use weak chiral potentials such that the orientation of chiral ligands does not change the magnitude of $\boldsymbol{\mu}_{ai}$ but does lead to changes in the angle, ϕ. Taking these results together with eq 6 implies that the orientation dependence of the rotational strength is due to changes in ϕ. In achiral systems, the electric and magnetic dipole vectors are orthogonal, $\phi = \pi/2$, and the rotatory strength vanishes.[22] But chiral ligands perturb the direction of the magnetic dipole away from orthogonality such that $\phi = \pi/2 \pm \delta\phi$, with $\delta\phi$ a small angle that depends on the orientation of the ligands. Some orientations correspond to positive values of $\delta\phi$ while others to negative values, giving rise to an opposite CD response for the same absolute stereochemistry, as depicted in Figure 5.

This analysis applies to a single quasiparticle transition. To delineate the role of ϕ on the observed CD spectra, one has to consider that each optical excitation should be represented by an admixture of quasiparticle transitions and that the overall CD spectrum is a combination of many such excitonic transitions. This complexity guides us toward qualitative intuitive predictions. Two general conclusions can be stated. First, we anticipate that disorder of the ligand orientations, either on a single QD or across an ensemble of dots, will decrease the overall CD signal as positive and negative peaks undergo cancellations. Directly inferred from this is that ordered configurations of chiral QDs will have enhanced CD signals, suggesting that the CD response could report on the degree of ligand shell order (see Figure S9).

Recent interest in the optical activity of QDs has raised several questions regarding the CD line shape and its dependence on size and shape. To address this, we developed an approach to induce chirality by surface ligands within the atomistic pseudopotential model, including electron−hole correlations. We applied the formalism to calculate the size- and orientation-dependent CD spectra for CdSe nanocrystals of varying sizes. We find that the origin of the bisignate line shape is due to many nondegenerate excitonic transitions of opposing angular momenta that combine to form the characteristic CD features. In addition, we investigated the dependence of the CD response on ligand orientation and found that the relative orientation of chiral ligands modulates the sign, magnitude, and apparent peak locations of the CD spectrum. We conclude that QDs exhibit flexible CD line shapes based on the precise orientation of passivating ligands. This suggests that chiral ligand tags could enable experimental studies of the order−disorder transition of ligand shells on colloidal semiconductor nanocrystals, lighting the way for chiroptical control.

■ ASSOCIATED CONTENT

Supporting Information

The Supporting Information is available free of charge at https://pubs.acs.org/doi/10.1021/acs.jpclett.4c01682.

Pseudopotential parameters; GitHub repository with source code, quantum dot configurations, and raw data

https://doi.org/10.1021/acs.jpclett.4c01682
J. Phys. Chem. Lett. 2024, 15, 7863−7869

files; induced CD convergence tests; method for canceling structural chirality; ligand-induced chirality of nanorods; CD spectra for increasingly ordered ligand configurations (PDF)

AUTHOR INFORMATION

Corresponding Author

Eran Rabani − *Department of Chemistry, University of California, Berkeley, Berkeley, California 94720, United States; The Sackler Center for Computational Molecular and Materials Science, Tel Aviv University, Tel Aviv, Israel 69978; Materials Sciences Division, Lawrence Berkeley National Laboratory, Berkeley, California 94720, United States;* orcid.org/0000-0003-2031-3525; Email: eran.rabani@berkeley.edu

Authors

Daniel Chabeda − *Department of Chemistry, University of California, Berkeley, Berkeley, California 94720, United States;* orcid.org/0000-0003-0152-7528

Stephen Gee − *Department of Materials, University of California, Santa Barbara, Santa Barbara, California 93106-5050, United States*

Complete contact information is available at: https://pubs.acs.org/10.1021/acs.jpclett.4c01682

Notes

The authors declare no competing financial interest.

ACKNOWLEDGMENTS

This work was supported by the U.S. Department of Energy, Office of Science, Office of Basic Energy Sciences, Materials Sciences and Engineering Division, under Contract No. DEAC02-05-CH11231 within the Fundamentals of Semiconductor Nanowire Program (KCPY23). Computational resources were provided in part by the National Energy Research Scientific Computing Center (NERSC), a U.S. Department of Energy Office of Science User Facility operated under Contract No. DEAC02-05CH11231. This material is based upon work supported by the National Science Foundation Graduate Research Fellowship Program under Grant No. DGE 2146752 (DC). Any opinions, findings, and conclusions or recommendations expressed in this material are those of the author(s) and do not necessarily reflect the views of the National Science Foundation. We thank Professor Ming Chen for helping develop the approach to compute the CD spectrum and for fruitful discussions. We also thank Drs. Assaf Ben-Moshe, John Philbin, and Daniel Weinberg for helpful discussions.

REFERENCES

(1) Alivisatos, A. P. Perspectives on the Physical Chemistry of Semiconductor Nanocrystals. *J. Phys. Chem.* **1996**, *100*, 13226−13239.

(2) Efros, A. L.; Rosen, M. The Electronic Structure of Semiconductor Nanocrystals. *Annu. Rev. Mater. Sci.* **2000**, *30*, 475−521.

(3) Liu, M.; Yazdani, N.; Yarema, M.; Jansen, M.; Wood, V.; Sargent, E. H. Colloidal Quantum Dot Electronics. *Nat. Electron.* **2021**, *4*, 548−558.

(4) Bukowski, T. J.; Simmons, J. H. Quantum Dot Research: Current State and Future Prospects. *Crit. Rev. Solid State and Mater. Sci.* **2002**, *27*, 119−142.

(5) Konstantatos, G.; Howard, I.; Fischer, A.; Hoogland, S.; Clifford, J.; Klem, E.; Levina, L.; Sargent, E. H. Ultrasensitive Solution-Cast Quantum Dot Photodetectors. *Nature* **2006**, *442*, 180−183.

(6) Hao, J.; Zhao, F.; Wang, Q.; Lin, J.; Chen, P.; Li, J.; Zhang, D.; Chen, M.; Liu, P.; Delville, M.-H.; He, T.; Cheng, J.; Li, Y. Optically Active CdSe/CdS Nanoplatelets Exhibiting Both Circular Dichroism and Circularly Polarized Luminescence. *Adv. Opt. Mater.* **2021**, *9*, 2101142.

(7) Cheng, J.; Hao, J.; Liu, H.; Li, J.; Li, J.; Zhu, X.; Lin, X.; Wang, K.; He, T. Optically Active CdSe-Dot/CdS-Rod Nanocrystals with Induced Chirality and Circularly Polarized Luminescence. *ACS Nano* **2018**, *12*, 5341−5350.

(8) Crassous, J.; Fuchter, M. J.; Freedman, D. E.; Kotov, N. A.; Moon, J.; Beard, M. C.; Feldmann, S. Materials for Chiral Light Control. *Nat. Rev. Mater.* **2023**, *8*, 365.

(9) Nozik, A. J. Quantum Dot Solar Cells. *Physica E Low Dimens. Syst. Nanostruct.* **2002**, *14*, 115−120.

(10) Coe, S.; Woo, W.-K.; Bawendi, M.; Bulović, V. Electroluminescence from Single Monolayers of Nanocrystals in Molecular Organic Devices. *Nature* **2002**, *420*, 800−803.

(11) Medintz, I. L.; Uyeda, H. T.; Goldman, E. R.; Mattoussi, H. Quantum Dot Bioconjugates for Imaging, Labelling and Sensing. *Nat. Mater.* **2005**, *4*, 435−446.

(12) Xia, Y.; Zhou, Y.; Tang, Z. Chiral Inorganic Nanoparticles: Origin, Optical Properties and Bioapplications. *Nanoscale* **2011**, *3*, 1374−1382.

(13) Baimuratov, A. S.; Rukhlenko, I. D.; Turkov, V. K.; Baranov, A. V.; Fedorov, A. V. Quantum Dot Supercrystals for Future Nanophotonics. *Sci. Rep.* **2013**, *3*, 1727.

(14) Economou, S. E.; Climente, J. I.; Badolato, A.; Bracker, A. S.; Gammon, D.; Doty, M. F. Scalable Qubit Architecture Based on Holes in Quantum Dot Molecules. *Phys. Rev. B* **2012**, *86*, 085319.

(15) Weiss, K. M.; Elzerman, J. M.; Delley, Y. L.; Miguel-Sanchez, J.; Imamoğu, A. Coherent Two-Electron Spin Qubits in an Optically Active Pair of Coupled InGaAs Quantum Dots. *Phys. Rev. Lett.* **2012**, *109*, 107401.

(16) Baimuratov, A. S.; Gun'ko, Y. K.; Baranov, A. V.; Fedorov, A. V.; Rukhlenko, I. D. Chiral Quantum Supercrystals with Total Dissymmetry of Optical Response. *Sci. Rep.* **2016**, *6*, 23321.

(17) Han, P.; Du, T.; Yang, X.; Zhao, Y.; Zhou, S.; Zhao, J. Optical Activity and Excitonic Characteristics of Chiral CdSe Quantum Dots. *J. Phys. Chem. Lett.* **2024**, *15*, 3249−3257.

(18) Ben-Moshe, A.; Teitelboim, A.; Oron, D.; Markovich, G. Probing the Interaction of Quantum Dots with Chiral Capping Molecules Using Circular Dichroism Spectroscopy. *Nano Lett.* **2016**, *16*, 7467−7473.

(19) Kuznetsova, V.; Gromova, Y.; Martinez-Carmona, M.; Purcell-Milton, F.; Ushakova, E.; Cherevkov, S.; Maslov, V.; Gun'ko, Y. K. Ligand-Induced Chirality and Optical Activity in Semiconductor Nanocrystals: Theory and Applications. *Nanophotonics* **2020**, *10*, 797−824.

(20) Tohgha, U.; Deol, K. K.; Porter, A. G.; Bartko, S. G.; Choi, J. K.; Leonard, B. M.; Varga, K.; Kubelka, J.; Muller, G.; Balaz, M. Ligand Induced Circular Dichroism and Circularly Polarized Luminescence in CdSe Quantum Dots. *ACS Nano* **2013**, *7*, 11094−11102.

(21) Baimuratov, A. S.; Rukhlenko, I. D.; Gun'ko, Y. K.; Baranov, A. V.; Fedorov, A. V. Dislocation-Induced Chirality of Semiconductor Nanocrystals. *Nano Lett.* **2015**, *15*, 1710−1715.

(22) Tepliakov, N. V.; Baimuratov, A. S.; Baranov, A. V.; Fedorov, A. V.; Rukhlenko, I. D. Optical Activity of Chirally Distorted Nanocrystals. *J. Appl. Phys.* **2016**, *119*, 194302.

(23) Tepliakov, N. V.; Vovk, I. A.; Shlykov, A. I.; Leonov, M. Y.; Baranov, A. V.; Fedorov, A. V.; Rukhlenko, I. D. Optical Activity and Circular Dichroism of Perovskite Quantum-Dot Molecules. *J. Phys. Chem. C* **2019**, *123*, 2658−2664.

(24) Gao, X.; Zhang, X.; Zhao, L.; Huang, P.; Han, B.; Lv, J.; Qiu, X.; Wei, S.-H.; Tang, Z. Distinct Excitonic Circular Dichroism between Wurtzite and Zincblende CdSe Nanoplatelets. *Nano Lett.* **2018**, *18*, 6665−6671.

(25) Ben Moshe, A.; Szwarcman, D.; Markovich, G. Size Dependence of Chiroptical Activity in Colloidal Quantum Dots. *ACS Nano* **2011**, *5*, 9034−9043.

(26) Ben-Moshe, A.; Maoz, B. M.; Govorov, A. O.; Markovich, G. Chirality and Chiroptical Effects in Inorganic Nanocrystal Systems with Plasmon and Exciton Resonances. *Chem. Soc. Rev.* **2013**, *42*, 7028−7041.
(27) Ben-Moshe, A.; Markovich, G. Chiral Ligand Induced Circular Dichroism in Excitonic Absorption of Colloidal Quantum Dots. *Isr. J. Chem.* **2012**, *52*, 1104−1110.
(28) Moloney, M. P.; Gun'ko, Y. K.; Kelly, J. M. Chiral Highly Luminescent CdS Quantum Dots. *Chem. Commun.* **2007**, 3900−3902.
(29) Hao, J.; Li, Y.; Miao, J.; Liu, R.; Li, J.; Liu, H.; Wang, Q.; Liu, H.; Delville, M.-H.; He, T.; Wang, K.; Zhu, X.; Cheng, J. Ligand-Induced Chirality in Asymmetric CdSe/CdS Nanostructures: A Close Look at Chiral Tadpoles. *ACS Nano* **2020**, *14*, 10346−10358.
(30) Boles, M. A.; Ling, D.; Hyeon, T.; Talapin, D. V. The Surface Science of Nanocrystals. *Nat. Mater.* **2016**, *15*, 141−153.
(31) Brown, P. R.; Kim, D.; Lunt, R. R.; Zhao, N.; Bawendi, M. G.; Grossman, J. C.; Bulović, V. Energy Level Modification in Lead Sulfide Quantum Dot Thin Films through Ligand Exchange. *ACS Nano* **2014**, *8*, 5863−5872.
(32) Toolan, D. T. W.; Weir, M. P.; Kilbride, R. C.; Willmott, J. R.; King, S. M.; Xiao, J.; Greenham, N. C.; Friend, R. H.; Rao, A.; Jones, R. A. L.; Ryan, A. J. Controlling the Structures of Organic Semiconductor Quantum Dot Nanocomposites Through Ligand Shell Chemistry. *Soft Matter* **2020**, *16*, 7970−7981.
(33) Wuister, S. F.; de Mello Donegá, C.; Meijerink, A. Luminescence Temperature Antiquenching of Water-Soluble CdTe Quantum Dots: Role of the Solvent. *J. Am. Chem. Soc.* **2004**, *126*, 10397−10402.
(34) Widmer-Cooper, A.; Geissler, P. Orientational Ordering of Passivating Ligands on CdS Nanorods in Solution Generates Strong Rod−Rod Interactions. *Nano Lett.* **2014**, *14*, 57−65.
(35) Peng, X.; Manna, L.; Yang, W.; Wickham, J.; Scher, E.; Kadavanich, A.; Alivisatos, A. P. Shape Control of CdSe Nanocrystals. *Nature* **2000**, *404*, 59−61.
(36) Widmer-Cooper, A.; Geissler, P. L. Ligand-Mediated Interactions between Nanoscale Surfaces Depend Sensitively and Nonlinearly on Temperature, Facet Dimensions, and Ligand Coverage. *ACS Nano* **2016**, *10*, 1877−1887.
(37) Calvin, J. J.; Brewer, A. S.; Alivisatos, A. P. The Role of Organic Ligand Shell Structures in Colloidal Nanocrystal Synthesis. *Nat. Synth.* **2022**, *1*, 127−137.
(38) Calvin, J. J.; Ben-Moshe, A.; Curling, E. B.; Brewer, A. S.; Sedlak, A. B.; Kaufman, T. M.; Alivisatos, A. P. Thermodynamics of the Adsorption of Cadmium Oleate to Cadmium Sulfide Quantum Dots and Implications of a Dynamic Ligand Shell. *J. Phys. Chem. C* **2022**, *126*, 12958−12971.
(39) Balan, A. D.; Olshansky, J. H.; Horowitz, Y.; Han, H.-L.; O'Brien, E. A.; Tang, L.; Somorjai, G. A.; Alivisatos, A. P. Unsaturated Ligands Seed an Order to Disorder Transition in Mixed Ligand Shells of CdSe/CdS Quantum Dots. *ACS Nano* **2019**, *13*, 13784−13796.
(40) Watson, B. R.; Ma, Y.-Z.; Cahill, J. F.; Doughty, B.; Calhoun, T. R. Probing Ligand Removal and Ordering at Quantum Dot Surfaces Using Vibrational Sum Frequency Generation Spectroscopy. *J. Colloid Interface Sci.* **2019**, *537*, 389−395.
(41) Morris-Cohen, A. J.; Malicki, M.; Peterson, M. D.; Slavin, J. W. J.; Weiss, E. A. Chemical, Structural, and Quantitative Analysis of the Ligand Shells of Colloidal Quantum Dots. *Chem. Mater.* **2013**, *25*, 1155−1165.
(42) Frederick, M. T.; Achtyl, J. L.; Knowles, K. E.; Weiss, E. A.; Geiger, F. M. Surface-Amplified Ligand Disorder in CdSe Quantum Dots Determined by Electron and Coherent Vibrational Spectroscopies. *J. Am. Chem. Soc.* **2011**, *133*, 7476−7481.
(43) Calvin, J. J.; Kaufman, T. M.; Sedlak, A. B.; Crook, M. F.; Alivisatos, A. P. Observation of Ordered Organic Capping Ligands on Semiconducting Quantum Dots via Powder X-Ray Diffraction. *Nat. Commun.* **2021**, *12*, 2663.
(44) Fisher, A. A. E.; Osborne, M. A.; Day, I. J.; Lucena Alcalde, G. Measurement of Ligand Coverage on Cadmium Selenide Nanocrystals and its Influence on Dielectric Dependent Photoluminescence Intermittency. *Commun. Chem.* **2019**, *2*, 1−9.
(45) Cai, J.; Liu, A.-A.; Shi, X.-H.; Fu, H.; Zhao, W.; Xu, L.; Kuang, H.; Xu, C.; Pang, D.-W. Enhancing Circularly Polarized Luminescence in Quantum Dots through Chiral Coordination-Mediated Growth at the Liquid/Liquid Interface. *J. Am. Chem. Soc.* **2023**, *145*, 24375−24385.
(46) Allenmark, S. Induced Circular Dichroism by Chiral Molecular Interaction. *Chirality* **2003**, *15*, 409−422.
(47) Jasrasaria, D.; Weinberg, D.; Philbin, J. P.; Rabani, E. Simulations of Nonradiative Processes in Semiconductor Nanocrystals. *J. Chem. Phys.* **2022**, *157*, 020901.
(48) Wang, L.-W.; Kim, J.; Zunger, A. Electronic Structures of [110]-Faceted Self-Assembled Pyramidal InAs/GaAs Quantum Dots. *Phys. Rev. B* **1999**, *59*, 5678−5687.
(49) Wang, L.-W.; Zunger, A. Pseudopotential Calculations of Nanoscale CdSe Quantum Dots. *Phys. Rev. B Condens.* **1996**, *53*, 9579−9582.
(50) Wang, L. W.; Zunger, A. Electronic Structure Pseudopotential Calculations of Large (.apprx.1000 Atoms) Si Quantum Dots. *J. Phys. Chem.* **1994**, *98*, 2158−2165.
(51) Rabani, E.; Hetényi, B.; Berne, B. J.; Brus, L. E. Electronic Properties of CdSe Nanocrystals in the Absence and Presence of a Dielectric Medium. *J. Chem. Phys.* **1999**, *110*, 5355−5369.
(52) Choi, J. K.; Haynie, B. E.; Tohgha, U.; Pap, L.; Elliott, K. W.; Leonard, B. M.; Dzyuba, S. V.; Varga, K.; Kubelka, J.; Balaz, M. Chirality Inversion of CdSe and CdS Quantum Dots without Changing the Stereochemistry of the Capping Ligand. *ACS Nano* **2016**, *10*, 3809−3815.
(53) Wall, M. R.; Neuhauser, D. Extraction, Through Filter-Diagonalization, of General Quantum Eigenvalues or Classical Normal Mode Frequencies from a Small Number of Residues or a Short-Time Segment of a Signal. I. Theory and Application to a Quantum-Dynamics model. *J. Chem. Phys.* **1995**, *102*, 8011−8022.
(54) Toledo, S.; Rabani, E. Very Large Electronic Structure Calculations Using an Out-of-Core Filter-Diagonalization Method. *J. Comput. Phys.* **2002**, *180*, 256−269.
(55) Brus, L. E. Electron−electron and electron-hole interactions in small semiconductor crystallites: The size dependence of the lowest excited electronic state. *J. Chem. Phys.* **1984**, *80*, 4403−4409.
(56) Rosenfeld, L. Quantenmechanische Theorie der Natürlichen Optischen Aktivität von Flüssigkeiten und Gasen. *Zeitschrift für Physik* **1929**, *52*, 161−174.
(57) Lin, K.; Jasrasaria, D.; Yoo, J. J.; Bawendi, M.; Utzat, H.; Rabani, E. Theory of Photoluminescence Spectral Line Shapes of Semiconductor Nanocrystals. *J. Phys. Chem. Lett.* **2023**, *14*, 7241−7248.
(58) Franceschetti, A.; Zunger, A. Direct Pseudopotential Calculation of Exciton Coulomb and Exchange Energies in Semiconductor Quantum Dots. *Phys. Rev. Lett.* **1997**, *78*, 915−918.
(59) Franceschetti, A.; Fu, H.; Wang, L. W.; Zunger, A. Many-Body Pseudopotential Theory of Excitons in InP and CdSe Quantum Dots. *Phys. Rev. B* **1999**, *60*, 1819−1829.
(60) Bester, G.; Nair, S.; Zunger, A. Pseudopotential Calculation of the Excitonic Fine Structure of Million-Atom Self-Assembled $In_{1-x}Ga_xAs$/GaAsQuantum Dots. *Phys. Rev. B* **2003**, *67*, 161306.
(61) Striolo, A.; Ward, J.; Prausnitz, J. M.; Parak, W. J.; Zanchet, D.; Gerion, D.; Milliron, D.; Alivisatos, A. P. Molecular Weight, Osmotic Second Virial Coefficient, and Extinction Coefficient of Colloidal CdSe Nanocrystals. *J. Phys. Chem. B* **2002**, *106*, 5500−5505.
(62) Jasieniak, J.; Smith, L.; Van Embden, J.; Mulvaney, P.; Califano, M. Re-examination of the Size-Dependent Absorption Properties of CdSe Quantum Dots. *J. Phys. Chem. C* **2009**, *113*, 19468−19474.

https://doi.org/10.1021/acs.jpclett.4c01682
J. Phys. Chem. Lett. 2024, 15, 7863−7869